THE JOURNAL OF BIOLOGICAL CHEMISTRY VOL. 281, NO. 23, pp. 16068–16077, June 9, 2006


# Regulation of Albumin Endocytosis by PSD95/Dlg/ZO-1 (PDZ) Scaffolds

## *INTERACTION OF $Na^+$-$H^+$ EXCHANGE REGULATORY FACTOR-2 WITH ClC-5**

Received for publication, November 23, 2005, and in revised form, March 23, 2006 Published, JBC Papers in Press, April 6, 2006, DOI 10.1074/jbc.M512559200

**Deanne H. Hryciw[‡], Jenny Ekberg[‡], Charles Ferguson[§], Aven Lee[‡], Dongsheng Wang[¶], Robert G. Parton[§], Carol A. Pollock[‖], Chris C. Yun[¶], and Philip Poronnik[‡1]**

*From the [‡]School of Biomedical Sciences, The University of Queensland, Brisbane, Queensland 4072, Australia, the [§]Institute for Molecular Bioscience and Centre for Microscopy and Microanalysis, The University of Queensland, Brisbane, Queensland 4072, Australia, the [‖]Kolling Institute, Royal North Shore Hospital, Department of Medicine, University of Sydney, New South Wales 2065, Australia, and the [¶]Department of Medicine, Division of Digestive Diseases, Emory University, Atlanta, Georgia 30322*

**The constitutive reuptake of albumin from the glomerular filtrate by receptor-mediated endocytosis is a key function of the renal proximal tubules. Both the $Cl^-$ channel ClC-5 and the $Na^+$-$H^+$ exchanger isoform 3 are critical components of the macromolecular endocytic complex that is required for albumin uptake, and therefore the cell-surface levels of these proteins may limit albumin endocytosis. This study was undertaken to investigate the potential roles of the epithelial PDZ scaffolds, $Na^+$-$H^+$ exchange regulatory factors, NHERF1 and NHERF2, in albumin uptake by opossum kidney (OK) cells. We found that ClC-5 co-immunoprecipitates with NHERF2 but not NHERF1 from OK cell lysate. Experiments using fusion proteins demonstrated that this was a direct interaction between an internal binding site in the C terminus of ClC-5 and the PDZ2 module of NHERF2. In OK cells, NHERF2 is restricted to the intravillar region while NHERF1 is located in the microvilli. Silencing NHERF2 reduced both cell-surface levels of ClC-5 and albumin uptake. Conversely, silencing NHERF1 increased cell-surface levels of ClC-5 and albumin uptake, presumably by increasing the mobility of NHE3 in the membrane and its availability to the albumin uptake complex. Surface biotinylation experiments revealed that both NHERF1 and NHERF2 were associated with the plasma membrane and that NHERF2 was recruited to the membrane in the presence of albumin. The importance of the interaction between NHERF2 and the cytoskeleton was demonstrated by a significant reduction in albumin uptake in cells overexpressing an ezrin binding-deficient mutant of NHERF2. Thus NHERF1 and NHERF2 differentially regulate albumin uptake by mechanisms that ultimately alter the cell-surface levels of ClC-5.**

The epithelial cells of the renal proximal tubule reabsorb large amounts of water, $Na^+$, $Cl^-$, $HCO_3^-$, $PO_4^-$, glucose, and amino acids from the glomerular filtrate (1). In addition to ions and small molecules, proteins such as albumin cross the glomerular barrier (2). Under normal conditions the tubular concentration of albumin in humans is ~4 mg/liter (3). This equates to 720 mg of albumin entering the kidneys each day and yet <30 mg of albumin is excreted per day, with the rest is constitutively reabsorbed in the proximal tubule by receptor-mediated endocytosis (2). This process involves the binding of albumin to the megalin/cubulin scavenger receptor, internalization of the complex, subsequent dissociation of the albumin from the receptor in the endosomes (2, 4), and finally degradation of albumin to its constitutive amino acids in the lysosomes, while megalin/cubulin is recycled back to the cell membrane (5).

A series of recent studies suggest that the endocytosis of albumin requires a macromolecular complex that includes the receptor, megalin/cubulin, the $Cl^-$ channel ClC-5, the $Na^+$-$H^+$ exchanger isoform 3 (NHE3),[2] and the v-type $H^+$-ATPase (2, 6, 7). The absolute requirement for megalin/cubulin is evident from the severe proteinuria seen in megalin/cubulin-deficient dogs (8). The functional basis for the obligate role of NHE3 in albumin uptake is less clear and may involve initiating the acidification of the nascent endosome by the electroneutral exchange of endosomal $Na^+$ for cytosolic $H^+$ (9, 10) or inhibiting fusion of the early endosome (10). This is demonstrated by reduced albumin uptake in the OK cell line when NHE3 is inhibited and the abolition of albumin uptake in NHE3-deficient OK cells (9, 11). These data are complemented by the finding of elevated levels of urinary protein in NHE3 knock-out mice (12). The situation with ClC-5 is more precise, because defective ClC-5 in Dent's disease patients results in proteinuria (13) as does ClC-5 knock-out in mice (14, 15). The proteinuria was hypothesized to result from reduced albumin uptake due to the lack of an anion shunt and failure of the endosomes to acidify (15), although new data showing that ClC-5 functions as a $Cl^-/H^+$ antiporter questions the role of ClC-5 as an anion shunt (16, 17). Another possible role played by ClC-5 is in mediating the protein-protein interactions that are involved in the assembly of the endocytic complex (6). This hypothesis is supported by data from the proximal tubules of ClC-5 knock-out mice and patients with Dent's disease where megalin is down-regulated and the v-$H^+$-ATPase is mistrafficked to the basolateral domain (18, 19). It is also clear that albumin uptake involves actin cytoskeleton acting as an anchoring point for the endocytic complex (20–22), because disruption of the cytoskeleton abolishes albumin uptake (21, 23). The presence of albumin causes actin clusters to form at the apical membrane that co-localize with the sites of albumin uptake (21). We have also shown that an interaction between ClC-5 and the actin-depolymerizing protein cofilin is required for albumin uptake (22). Thus, although significant progress has been made in identifying both ClC-5 and NHE3, as essen-

* This work was supported by grants from the National Health and Medical Research Council of Australia (to P. P., C. A. P., and R. G. P.). The costs of publication of this article were defrayed in part by the payment of page charges. This article must therefore be hereby marked "*advertisement*" in accordance with 18 U.S.C. Section 1734 solely to indicate this fact.

[1] To whom correspondence should be addressed. Tel.: 61-7-3365-2299; Fax: 61-7-3365-1766; E-mail: p.poronnik@uq.edu.au.

[2] The abbreviations used are: NHE3, $Na^+$-$H^+$ exchanger isoform 3; OK, opossum kidney cells; NHERF, $Na^+/H^+$ exchanger regulatory factor; GST, glutathione *S*-transferase; HRP, horseradish peroxidase; DMEM, Dulbecco's modified Eagle's medium; MBP, maltose binding protein; MOPS, 4-morpholinepropanesulfonic acid; GFP, green fluorescent protein; TR, Texas Red.

tial and therefore rate-limiting components in albumin uptake, we have little insight into the protein-protein interactions that direct the formation of the endocytic complex and anchor it to the cytoskeleton.

One class of proteins that is critically involved in the assembly of macromolecular complexes are PDZ module-containing scaffolds (24). The first PDZ scaffold protein described for an epithelial transporter was the $Na^+/H^+$ exchanger regulatory factor (NHERF, NHERF1, or EBP50) that was found to mediate the regulation of NHE3 by cAMP in the proximal tubule (25). Subsequently, a second protein, NHERF2 (or E3KARP), was also identified as a binding partner for NHE3 (26). NHERF1 and NHERF2 contain tandem PDZ modules and a C-terminal ezrin binding domain that can anchor the complex to the underlying actin cytoskeleton (24). Typically, PDZ modules bind to PDZ binding motifs in the extreme C terminus of target proteins, but they can also bind to internal sequences and lipids (27) as well as also forming homo- and heterodimers (28).

NHERF1 and NHERF2 share only 44% homology with most sequence conservation in their PDZ modules (26). Significantly, they display pronounced spatial heterogeneity in the proximal tubule with reports in both mouse and human (29–31) showing that NHERF1 is strongly expressed in the microvilli, while NHERF2 is primarily localized at the base of the microvilli in the vesicle-rich domains (29–31). NHERF proteins clearly have the capacity to nucleate the formation of functional complexes at the plasma membrane (30, 32) and restrict the mobility of plasma membrane proteins, such as NHE3 (33, 34). Thus the organized subcellular distribution of NHERF1/2 is speculated to play a role in the specific interactions that mediate the physiological regulation of transporter function (31). The current study was therefore undertaken to investigate the potential involvement of NHERF1/2 in albumin uptake and whether this involved interactions with ClC-5, a key component of the albumin endocytic complex.

## EXPERIMENTAL PROCEDURES

*Materials and Antibodies*—Anti-NHERF1 (35), anti-NHERF2 (20) and anti-ClC-5 antibody have been previously described (22, 36). Anti-GST conjugated to horseradish peroxidase (HRP) was provided by Amersham Biosciences, and anti-MBP conjugated to HRP was provided by New England Biolabs. Secondary antibody conjugated to rhodamine was obtained from Calbiochem. Secondary antibodies conjugated to HRP were from Pierce.

*Cell Culture*—The opossum kidney (OK) cell line was obtained from Dr. Daniel Markovich (University of Queensland), and the cells were maintained in DMEM/Ham's F-12 (DMEM/F-12) media supplemented with 10% fetal bovine serum, penicillin/streptomycin and incubated at 37 °C in 5% $CO_2$. For experimental protocols, OK cells were seeded at confluence and grown for 5 days. Two days prior to experimentation, cells were incubated in DMEM/F-12 with 5 mM glucose medium lacking serum. HEK293 cells were maintained in DMEM media supplemented with 10% fetal bovine serum, penicillin/streptomycin, and incubated at 37 °C in 5% $CO_2$.

*Characterization of NHERF2 in OK Cells*—RNA was extracted from OK cells and HEK-293 (control) cells using TRIzol reagent (Invitrogen) according to the manufacturer's instructions. Total RNA (2 $\mu$g) was treated with DNase (Promega) and then reverse-transcribed using Superscript III (Invitrogen). NHERF2 was amplified using primers described previously (37). For Western blot detection, Triton X-100-soluble fractions of OK cells (40 $\mu$g) were separated on a 10% SDS-PAGE gel and transferred to a nitrocellulose membrane. NHERF2 was then detected using a rabbit polyclonal anti-NHERF2 antibody (1:10,000 dilution). The cellular distribution of NHERF2 was determined by confocal microscopy using the NHERF2 antibody (1:100) and a secondary anti-rabbit antibody conjugated to rhodamine (Calbiochem, 1:40).

*GST Pull-down Assay*—Generation of the GST fusion proteins containing NHERF1 and NHERF2, the individual PDZ domains NHERF2 PDZ1 (PDZ1), NHERF2 PDZ2 (PDZ2) and NHERF2 C terminus (C-term) and the C terminus of ClC-5 (GST-ClC-5) have been previously described (19, 34). The GST fusion proteins were produced as described previously using the GST purification kit (Amersham Biosciences) following the manufacturer's instructions (22). In brief, the bacteria were induced to produce GST fusion protein with IPTG (1 mM), cells lysed and the GST fusion protein purified using a glutathione Sepharose 4B column. For the pulldown assay, 50 $\mu$g of GST or GST fusion protein were incubated with glutathione-Sepharose 4B beads (Amersham Biosciences) for 3 h at 4 °C. The beads were then washed, centrifuged, and incubated with ~1 mg of lysate from OK cells at 4 °C for 18 h. The beads were washed repeatedly, and the samples were eluted into Laemmli gel sample buffer. Samples were resolved on SDS-PAGE gel and transferred to nitrocellulose membranes. Western blotting was performed using the appropriate antibody, and the blots were detected using secondary antibodies conjugated to HRP and the SuperSignal West Pico Substrate (Pierce). In addition, 50 $\mu$g of GST fusion proteins was transferred to a nitrocellulose membrane and probed with anti-GST conjugated to HRP to demonstrate an equal amount of protein in the reaction. The protein was detected using the SuperSignal West Pico Substrate (Pierce).

*MBP Pull-down Assay*—The C terminus of ClC-5 was subcloned into pMAL-c2x (New England Biolabs). A mutant that lacked the final five amino acids (D741X) was generated using site-directed mutagenesis as described previously (38). Both plasmids were used to transform BL-21 component cells. The fusion protein containing the C terminus of ClC-5 fused to MBP (MBP-ClC-5) and the D741X mutant (MBP-ΔPDZ) were induced with isopropyl 1-thio-$\beta$-D-galactopyranoside (1 mM), the cells were lysed, and the fusion protein was isolated using an amylose column. For the direct interaction assay, 5 $\mu$g of MBP-ClC-5, MBP-ΔPDZ, or MBP alone as a control was incubated with amylose beads for 3 h at 4 °C. GST-NHERF2 (300 ng) was then added to the complex, and the mixture was incubated overnight. The complex was pelleted and washed four times with buffer containing 1% Triton X-100. The samples were suspended in Laemmli gel sample buffer, separated on a 10% SDS-PAGE gel, and transferred to nitrocellulose membranes. Western blotting was performed using the anti-NHERF2 antibody, and the blots were detected using secondary antibodies conjugated to HRP and the SuperSignal West Pico Substrate (Pierce). As a further control, 50 $\mu$g of MBP fusion proteins was transferred to a nitrocellulose membrane and probed with anti-MBP conjugated to HRP to demonstrate an equal amount of protein in the reaction. The protein was detected using the SuperSignal West Pico Substrate (Pierce).

*Immunoprecipitation*—Protein-A-agarose beads (Roche Applied Science) were used for immunoprecipitation experiments using the manufacturer's protocol. Briefly, OK cells were lysed in lysis buffer (50 mM Tris-HCl, pH 7.5, 150 mM NaCl, 1% Triton X-100, and Complete protease inhibitors (Roche Applied Science)). 50 $\mu$l of Protein-A-agarose was incubated with the lysate for 3 h at 4 °C. The pre-cleared lysate was then incubated with anti-NHERF1 or anti-NHERF2 antibodies at 4 °C overnight. Protein-A-agarose (50 $\mu$l) was added to the sample, and the mixture was incubated for 3 h at 4 °C. The pelleted beads were then washed three times in 500 $\mu$l of wash buffer (50 mM Tris-HCl, pH 7.5, 500 mM NaCl, 0.1% Triton X-100), and the samples were eluted into Laemmli gel sample buffer, separated on a 5% SDS-PAGE gel, and then transferred to nitrocellulose membranes. Western blotting was performed with anti-

ClC-5 antibody as previously described (22). As a further control, 50 $\mu$g of OK cell lysate was resolved on SDS-PAGE gel transferred to a nitrocellulose membrane and probed with anti-ClC-5, anti-NHERF1, and anti-NHERF2 to demonstrate equal loading of the lysate in each reaction.

*Electrophysiological Recording of ClC-5 Currents in Xenopus oocytes*—Capped RNA (cRNA) transcripts encoding the full-length ClC-5 and NHERF2 were synthesized using the mMESSAGE mMACHINE *in vitro* transcription kit (Ambion). *Xenopus laevis* stage V–VI oocytes were treated with collagenase (Type I, Sigma) for defolliculation. The oocytes were then injected with cRNA for ClC-5 (5 ng/oocyte) in the absence and presence of the cRNA encoding NHERF2 (10 ng/oocyte) or water as a control. The oocytes were incubated at 18 °C in ND96 solution (96 mM NaCl, 2 mM KCl, 1 mM $CaCl_2$, 1 mM $MgCl_2$, 5 mM HEPES, 5 mM pyruvic acid, and 50 $\mu$g/ml gentamicin, pH 7.5) prior to recording. Three days after cRNA injection, membrane currents were recorded from oocytes using the two-electrode (virtual ground circuit) voltage clamp technique using microelectrodes filled with 3 M KCl. All recordings were made at room temperature (20–23 °C) using ND96 solution. Using a GeneClamp 500B amplifier and pCLAMP 8 software (Axon Instruments Inc., Union City, CA), data were low pass-filtered at 1 kHz, digitized at 10 kHz, and leak-subtracted on-line using a -P/8 protocol and analyzed offline. Inward $Cl^-$ currents mediated by ClC-5 were generated by holding the cells at −70 mV and applying 100-ms step depolarizations to membrane potentials from −30 mV to +80 mV. Statistical significance was determined using an unpaired *t* test (95% confidence interval).

*Electron Microscopy*—Cells were fixed with 8% (w/v) paraformaldehyde in phosphate-buffered saline and then processed for frozen sectioning according to published methods (39). Thawed sections were labeled with antibodies to NHERF1 or NHERF2 followed by 10 nm Protein A-gold (University of Utrecht).

*Transfections and Plasmid DNA*—OK cells were transiently transfected with either a wild-type-NHERF1, NHERF2, dominant negative-NHERF1 lacking the ezrin binding domain (NHERF-1ΔEZR), NHERF2 (NHERF-1ΔEZR), or control pCDNA3 plasmid. The ezrin binding domain links the NHERF proteins to the actin cytoskeleton (24). In addition, cells were transfected with the silencing RNA construct pSHAG (40) containing OK NHERF1-specific sequences (EBP114: 5′-CCAACGAGCCGGGCTCCACCAGGCCGGAT-3′ and EBP248: 5′-GTCGACCACCAGCAGGCGCACGGCGTTG-3′) and human NHERF2-specific sequences (pSHAG 274: 5′-ACGGCGTCAACGTGGAGGGCGAGACGCA-3′ and pSHAG 361: 5′-CCGAAGCCAGACTGGGCACACACCGGCAG-3′) or the control vector (pSHAG-FF that contains small interference RNA against firefly luciferase). All transfections were performed using Fugene (Roche Applied Science) or Effectene (Qiagen), following the manufacturers' protocol.

*Albumin Uptake*—We used standard albumin uptake methods in OK cells, a cell line commonly used for the study of proximal tubule albumin uptake (22, 41, 42). For transfected cells, control (mock transfected with vector) OK cells or cells transfected with the various constructs were grown in 48-well plates for 7 days (21, 22, 36, 43). To study the effect of cAMP on albumin uptake, cells were preincubated with 8-Br-cAMP (100 $\mu$M) for 1 h. To determine albumin uptake, cells were exposed to 50 $\mu$g/ml albumin conjugated to Texas Red (Molecular Probes) under the different conditions for 120 min (22). As a control to determine the level of endocytosis dependent on the intact cytoskeleton, some cells were pre-treated with cytochalasin B (1.5 $\mu$M) for 60 min before exposure to TR-albumin. Nonspecific binding was determined in cells exposed to albumin for 1 min. At the end of the uptake period, cells were washed in HEPES buffer, pH 6 at 4 °C, and then lysed in MOPS buffer (20 mM MOPS with 0.1% Triton X-100). The TR-albumin fluorescence was determined using a Fusion spectrophotometer (Hewlett Packard, Blackburn, Victoria, Australia) at 580 nm excitation and 630 nm emission wavelengths. TR-albumin uptake was standardized to total cellular protein, and the amount of fluorescence per microgram of cellular protein was adjusted for background.

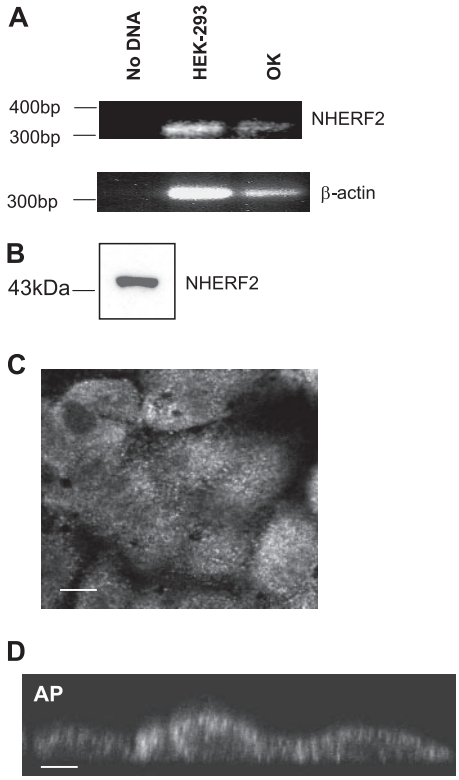


FIGURE 1. **NHERF2 is endogenously expressed in OK cells.** *A*, reverse transcription-PCR showing the presence of a 330-bp product that corresponds to NHERF2 in OK and control (HEK) cells, as well as the β-actin control. *B*, Western blot analysis showing a single band of 43 kDa corresponding to the NHERF2 protein in OK cells. *C*, X-Y confocal scan showing NHERF2 at the plane of the apical membrane (*scale bars* = 10 $\mu$m). *D*, X-Z confocal scan showing that NHERF-2 is predominantly cytosolic at the apical domain of OK cells.

*Cell-surface Biotinylation*—Cell-surface biotinylation was used to detect the levels of ClC-5 in the plasma membrane and the levels of NHERF1 and NHERF2 associated with the plasma membrane. OK cells were transiently transfected with pSHAG-FF, EBP114, EBP248, pSHAG 274, and pSHAG361 as described above. The cell-surface proteins were biotinylated as described previously (36). Briefly, confluent OK cell monolayers were washed three times in cold phosphate-buffered saline then biotinylated with 1.22 mg/ml EZ-Link NHS-SS-Biotin (Pierce) at 4 °C with gentle agitation. Monolayers were washed three times in cold phosphate-buffered saline, and the cells were lysed in lysis buffer. The biotinylated proteins were isolated by binding to ImmunoPure immobilized streptavidin (Pierce) for 15 min on ice. The beads were pelleted, and the supernatant that contained the cytoplasmic (unbiotinylated) fraction was recovered by centrifugation at 4500 × *g* for 6 min at 4 °C. The membrane (biotinylated) fraction was washed, and the pellet was suspended in Laemmli sample buffer. An equal protein amount of the biotinylated fractions and whole cell fractions were resolved on a 5% SDS-PAGE gel, and then transferred to nitrocellulose. Western blotting was performed with the anti-ClC-5, anti-NHERF1, and anti-NHERF2 antibodies as described above.

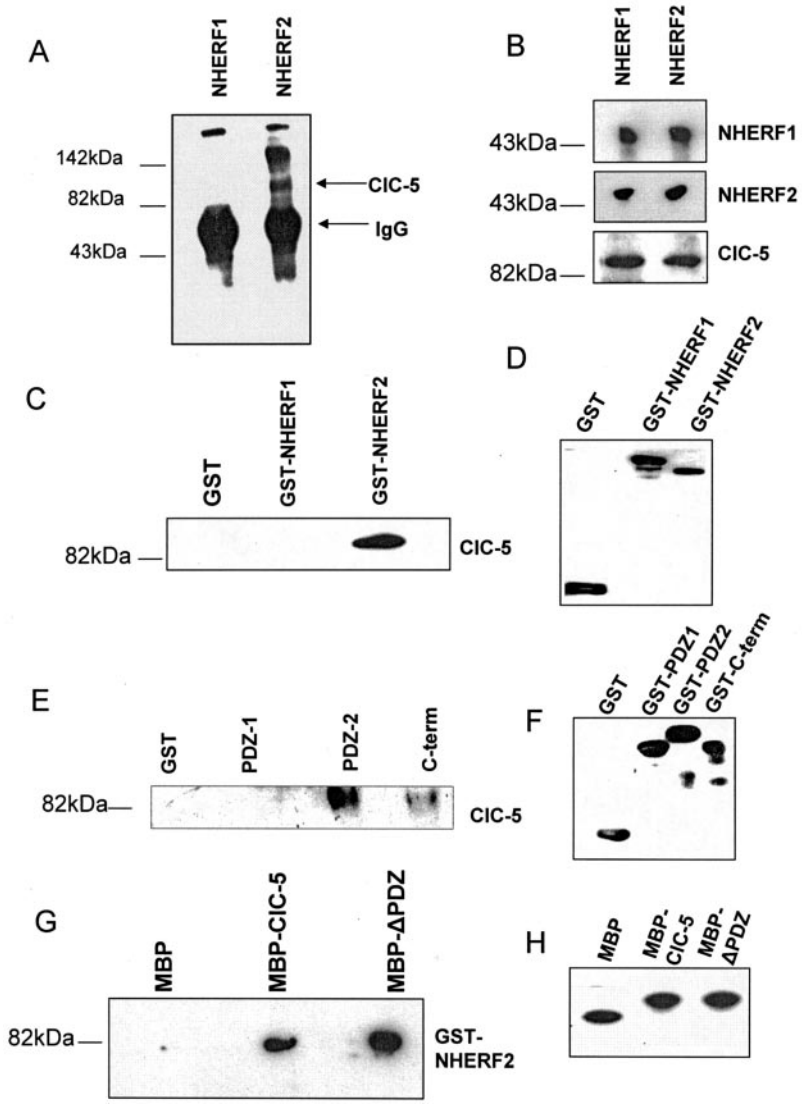


FIGURE 2. **ClC-5 interacts with NHERF2 *in vitro* and *in vivo*.** *A*, Western blot of NHERF1/2 co-immunoprecipitates probed with anti-ClC-5 antibody showing that ClC-5 binds to NHERF2 and not NHERF1 *in vivo*. The high molecular weight band is a putative ClC-5 dimer. *B*, Western blot of ClC-5, NHERF1, and NHERF2 showing equal amounts of these proteins in each reaction. *C*, Western blot of OK cell lysate incubated with GST-NHERF1/2 shows that ClC-5 binds to NHERF2 and not NHERF1 *in vitro*. *D*, Western blot of GST, GST-NHERF1, and GST-NHERF2 demonstrates equal amounts of the fusion proteins in the reaction. *E*, GST pull-down assays with NHERF2 functional domains shows that ClC-5 binds to PDZ of NHERF2. *F*, Western blot of GST, GST-PDZ1, GST-PDZ2, and GST-C-term showing equal amounts of the fusion proteins in the reaction. *G*, MBP, MBP-ClC-5, and MBP-ΔPDZ were incubated with GST-NHERF2. Both MBP-ClC-5 and MBP-ΔPDZ bind to GST-NHERF2. *H*, Western blot of MBP, MBP-ClC-5, and MBP-ΔPDZ showing equal amounts of the fusion proteins in the reaction.

*Confocal Microscopy*—Albumin uptake in OK cells transfected with the silencing RNA against NHERF1/2 was performed as previously described (21). Briefly, cells were seeded onto glass coverslips, transiently transfected with the NHERF-silencing RNA plasmids and GFP. Confluent monolayers of OK cells were exposed to 1 mg/ml TR-albumin for 20 min. All cells were fixed in 4% paraformaldehyde and were analyzed by confocal microscopy. Cells were analyzed by confocal microscopy using a Zeiss LSM 510 Meta confocal microscope with Plan-Apochromat 63×, 1.4 numerical aperture objective. GFP was excited at 488 nm, and emission was measured at 515 ± 15 nm. TR-albumin was excited at 543 nm and emission measured at 570 nm.

*Quantification of Results and Statistical Analysis*—Densitometric analysis of the Western blot data was performed using Fujifilm ScienceLab 99 Image Gauge (version 3.3). Statistical analyses of the data were performed using a two-tailed Student's paired *t* test or analysis of variance where appropriate with a $p$ value of $<0.05$ considered significant.

## RESULTS

*Distribution of NHERF2 in OK Cells*—It has been reported previously that some clones of OK cells express NHERF1 but not NHERF2 (30, 37, 44). It was therefore essential to confirm that the OK cells used in the current study did express NHERF2. Reverse transcription-PCR using NHERF2-specific primers (37) performed on mRNA isolated from OK cells clearly showed the presence of the message for NHERF2 (Fig. 1*A*), and Western blot analysis on cell lysate demonstrated the presence of NHERF2 protein (Fig. 1*B*). Finally, confocal analysis of confluent OK cells revealed abundant cytosolic staining for NHERF2 that was more pronounced at the apical domain (Fig. 1, *C* and *D*), a distribution that is similar to that reported for NHE3 and ClC-5 (45, 46).

*ClC-5 Interacts with NHERF2 but Not NHERF1*—To demonstrate *in vivo* and *in vitro* interactions between ClC-5 and NHERF1/2 we first performed co-immunoprecipitations using NHERF1- and NHERF2-specific antibodies. We found that NHERF2 but not NHERF1 antibody precipitated ClC-5 from OK cell lysates (Fig. 2*A*). Lysate controls showed equal amounts of NHERF1, NHERF2, and ClC-5 in the reactions (Fig. 2*B*). This interaction was confirmed by using GST fusion proteins of NHERF1/2 to show that only NHERF2 could pull down ClC-5 from OK cell lysate (Fig. 2*C*). Fusion protein controls showed equal amounts of GST, GST-NHERF1, and GST-NHERF2 in the reactions (Fig. 2*D*). Further experiments were then performed with GST fusion proteins expressing the individual functional domains (PDZ1, PDZ2, and C terminus) of NHERF2 to show that ClC-5 bound to the second PDZ domain (Fig. 2*E*). Again, fusion protein controls showed

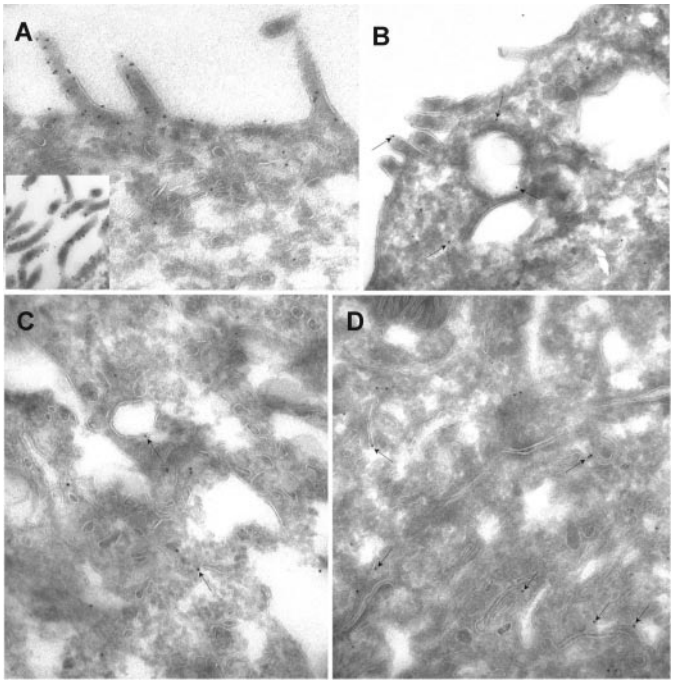


FIGURE 3. **Distribution of NHERF1 and NHERF2 in polarized OK cells.** *A*, electron micrograph showing that NHERF1 is primarily expressed in the microvilli of OK cells (*inset* shows cluster of microvilli). *B–D*, electron micrographs showing that NHERF2 (*arrows*) is primarily associated with intracellular membranes below the apical membrane. *Panel B* shows a section through the apical surface of the cell, whereas *C* and *D* show glancing sections through the subapical region (note the subapical junctional complexes between adjacent cells in *D*).

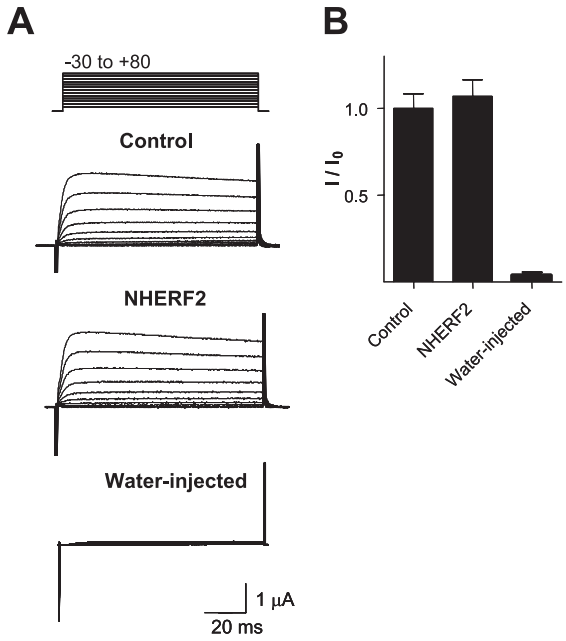


FIGURE 4. **NHERF2 does not alter the current amplitude of ClC-5.** *A*, representative $Cl^-$ currents recorded from oocytes expressing ClC-5 in the absence (control) and presence of NHERF2 and water injected. To evoke inward $Cl^-$ currents, oocytes were held at −70 mV and step-depolarized to voltages between −30 and +80 mV in 10-mV increments. *B*, *bar graph* representing the $Cl^-$ current amplitude at +80 mV recorded from oocytes that were water injected (control), expressing ClC-5 alone and in combination with NHERF2 (*I*) relative to the average of control $Cl^-$ current amplitude (recorded from oocytes expressing only ClC-5) ($I_0$). Data are expressed as the mean ± S.E. of 38–39 oocytes from three separate batches.

equal amounts of GST, GST-PDZ 1, GST-PDZ2, and GST-C-term in the reactions (Fig. 2*F*). Protein-protein interactions detected using GST-pull-downs in cell lysates may occur as a result of accessory proteins. Therefore, to demonstrate a direct interaction between CLC-5 and NHERF2, we incubated MBP-ClC-5 with GST-NHERF2 *in vitro*. The MBP-ClC-5 was recovered and then run on a Western blot that was probed with anti-NHERF2. GST-NHERF2 incubated with MBP alone as a negative control showed no interaction, whereas in the lane with MBP-ClC5 there was a single band at ~80 kDa that corresponds to GST-NHERF2 (Fig. 2*G*). Interestingly, ClC-5 has a potential PDZ binding motif (*ESIL*FN) from −6 to −3 position in the last 6 amino acids of the C terminus that could potentially interact with PDZ proteins. Deletion of the 5 terminal amino acids of ClC-5 (MBP-ΔPDZ) did not alter the binding to NHERF2 (Fig. 2*G*), demonstrating that NHERF2 binds to an internal motif in the ClC-5 cytosolic tail (see Ref. 6). Fusion protein controls showed equal amounts of MBP, MBP-ClC-5, and MBP-ΔPDZ in the reactions (Fig. 2*H*).

*Subcellular Localization of NHERF1 and NHERF2 in OK Cells*—Electron microscopy revealed that, in OK cells, NHERF1 was localized predominantly to the brush border membrane (Fig. 3*A* and *inset*), whereas NHERF2 was associated primarily with intracellular membranes in the proximity of the apical membrane, a distribution pattern similar to that observed for NHERF2 in the mouse and human (Fig. 3, *B–D*).

*Effect of NHERF2 on ClC-5 Currents*—ClC-5 binds to the PDZ2 module of NHERF2, which could leave the PDZ1 domains free to dimerize, thereby concentrating ClC-5 protein at the cell surface. To establish whether NHERF2 had any effect on the cell-surface density of ClC-5, we co-injected *Xenopus* oocytes with cRNA for ClC-5 and NHERF2 and performed standard two-electrode voltage clamp experiments. The presence of NHERF2 caused no change in the size of the currents mediated by ClC-5 in the presence of NHERF2 ($n = 3$, 38–39 oocytes, Fig. 4, *A* and *B*).

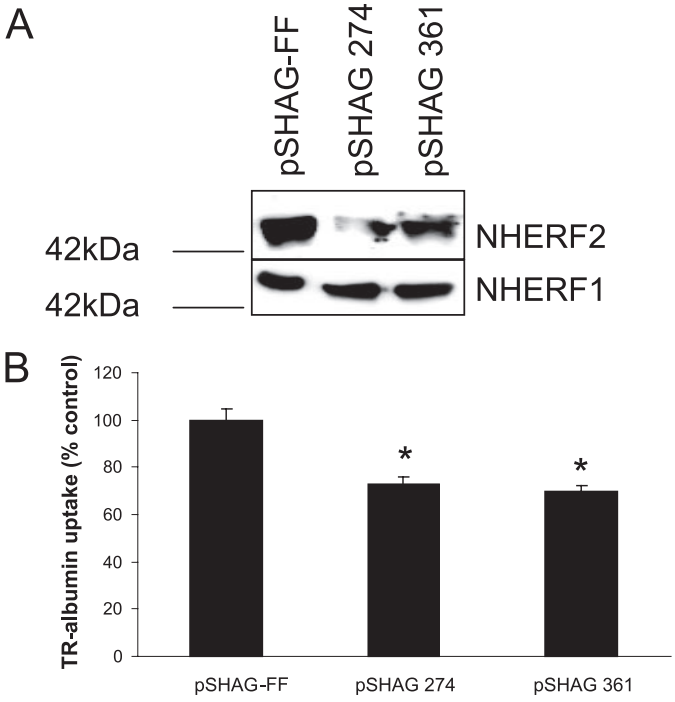


FIGURE 5. **Silencing NHERF2 inhibits albumin uptake.** *A*, Western blot analysis of cells transfected with pSHAG 274 and pSHAG 361 shows a decrease in NHERF2 expression compared with cells transfected with vector control (pSHAG-FF). No change in NHERF1 protein expression was observed. *B*, silencing NHERF2 with pSHAG 274 and pSHAG 361 causes a significant decrease in albumin endocytosis relative to cells transfected with vector (pSHAG-FF) control (*, $p < 0.05$; $n = 4$).

*Roles of NHERF2 and NHERF1 in Albumin Endocytosis*—If the interaction between ClC-5 and NHERF2 is physiologically relevant, silencing endogenous NHERF2 should affect the rate of albumin uptake because

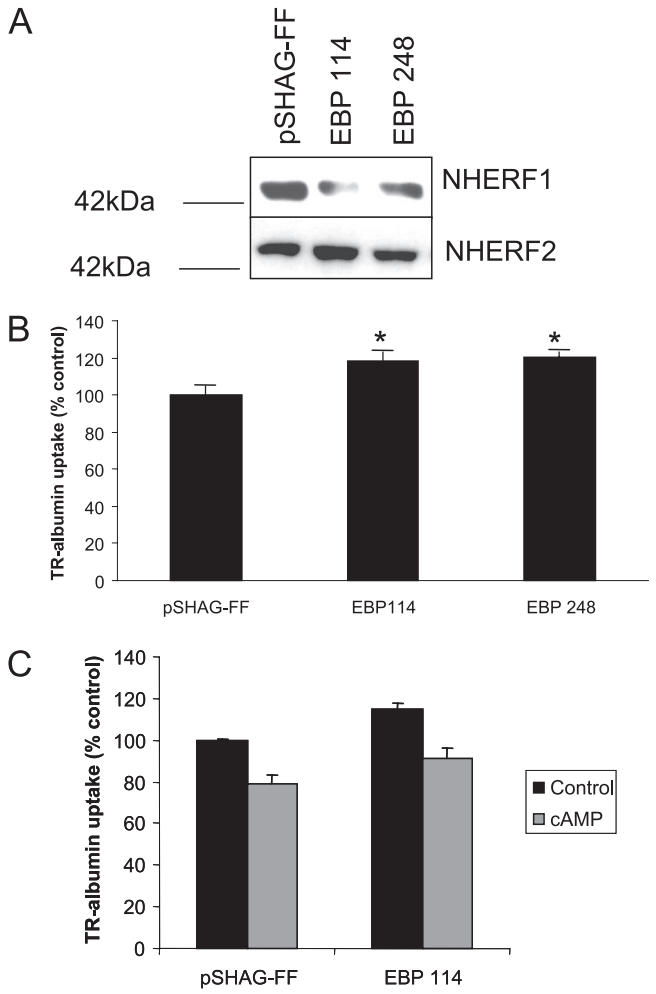


FIGURE 6. **Silencing NHERF1 increases albumin uptake but does not involve cAMP.** *A*, Western blot analysis of cells transfected with EBP114 and EBP248 shows a decrease in NHERF1 expression compared with cells transfected with vector control (pSHAG-FF). No changes in NHERF2 protein expression were observed. *B*, in cells where NHERF1 was silenced with either EBP114 or EBP248 there was a significant increase in albumin endocytosis relative to cells transfected with vector control (pSHAG-FF) (*, $p < 0.05$; $n = 4$). *C*, pre-treatment of OK cells with 8-Br-cAMP (100 $\mu$M) causes a significant decrease in albumin uptake in both control cells (pSHAG-FF) and cells transfected with EBP114. Despite the increase in albumin uptake when NHERF1 was silenced, there was no change in the percent inhibition by 8-Br-cAMP. The percent inhibition of total albumin uptake was 21.9 ± 3% for the pSHAG-FF and 21.8 ± 3% when NHERF1 was silenced ($n = 3$).

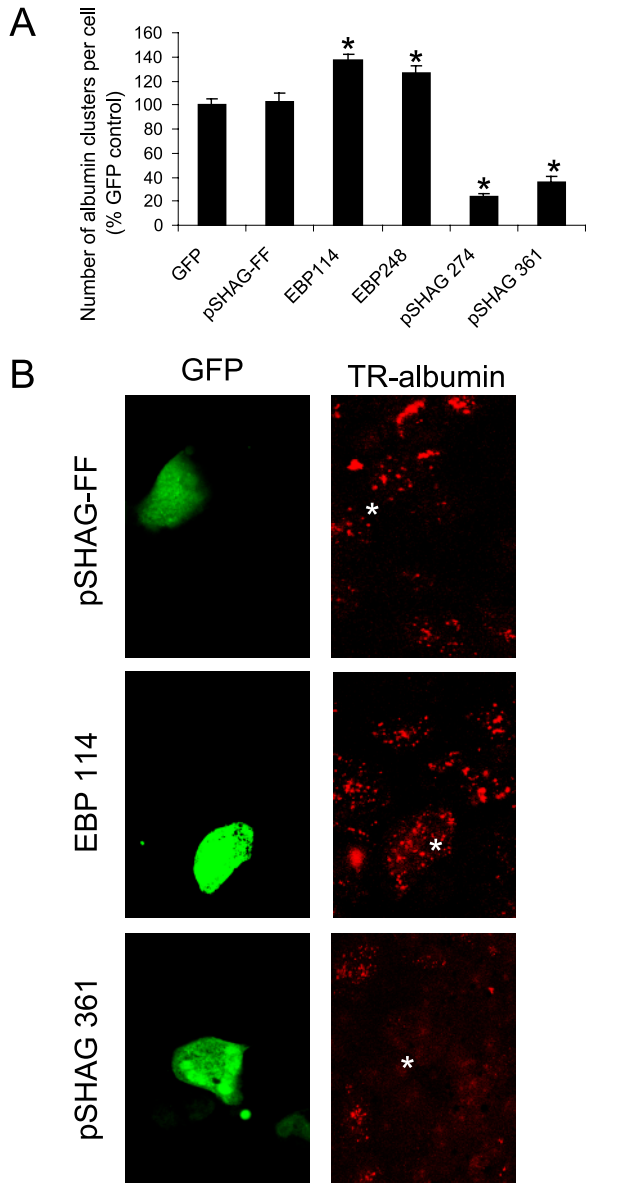


FIGURE 7. **Silencing NHERF1/2 alters the number of albumin endocytic vesicles.** OK cells co-transfected with silencing constructs and GFP were exposed to TR-albumin (50 $\mu$g/ml) for 2 h, and confocal images were obtained. The number of albumin clusters per cell was then calculated to determine the effects of silencing NHERF1/2 on albumin uptake in single cells. *A*, in cells silenced for NHERF1 (EBP114 and EBP248) there was a significant increase in albumin clusters per cell (136.9 ± 0.9% and 126.3 ± 1.0%, respectively; $n = 3$) compared with cells transfected with GFP and pSHAG-FF (102.5 ± 1.3%; *, $p < 0.05$; $n = 3$). In cells transfected with GFP and pSHAG274 or pSHAG361 there was a significant decrease in albumin clusters per cell (23.8 ± 0.5% and 35.4 ± 0.8%, respectively; *, $p < 0.05$; $n = 3$). *B*, dual wavelength confocal imaging of representative single cells showing changes in the number of albumin endocytic vesicles. The GFP channel indicating transfected cells (*left column*) and the corresponding TR-albumin uptake images (*right column*). Cells were transfected with either pSHAG-FF (control), EBP114 (NHERF1 silenced), or pSHAG361 (NHERF2 silenced).

of the obligate role of ClC-5 in albumin uptake. We therefore performed albumin uptake experiments on OK cells transiently transfected with plasmids expressing small interference RNA directed against NHERF2. We used two different silencing plasmids (pSHAG274 and pSHAG361) (47) that target different regions of the NHERF2 open reading frame, and both these plasmids caused significant reductions in endogenous NHERF2 to 64.0 ± 5.9% and 72.5 ± 7.5% of control values (Fig. 5*A*), whereas the levels of NHERF1 remained unchanged. Importantly, silencing of NHERF2 with either pSHAG274 or pSHAG361 resulted in significant decreases in TR-albumin uptake to 74 ± 3% and 67 ± 4%, respectively ($n = 3$, $p < 0.05$) of the control levels (pSHAG-FF) (Fig. 5*B*). As reported previously, the transfection efficiencies of OK cells in these experiments are typically of the order of ~50% (22), therefore, the ~30% reduction we observe in TR-albumin uptake by the total population of cells is a significant underestimate of the true reduction in TR-albumin uptake by those cells that express small interference RNA directed against NHERF2. This is confirmed in the confocal experiments performed on albumin uptake in single OK cells (*cf.* Fig. 7 below).

We next investigated the effects of silencing NHERF1 on albumin uptake. OK cells were transiently transfected with plasmids expressing small interference RNA (EBP114 and EBP248) against NHERF1 that resulted in a pronounced reduction in the levels of NHERF1 to 73.3 ± 5.7% and 65.6 ± 7.7% of control levels with no change in the levels of NHERF2 (Fig. 6*A*). When NHERF1 was silenced, there were significant increases in albumin uptake to 118 ± 6% compared with control for EBP114 and 120 ± 4% for EBP248 ($n = 3$, $p < 0.05$, Fig. 6*B*). Albumin

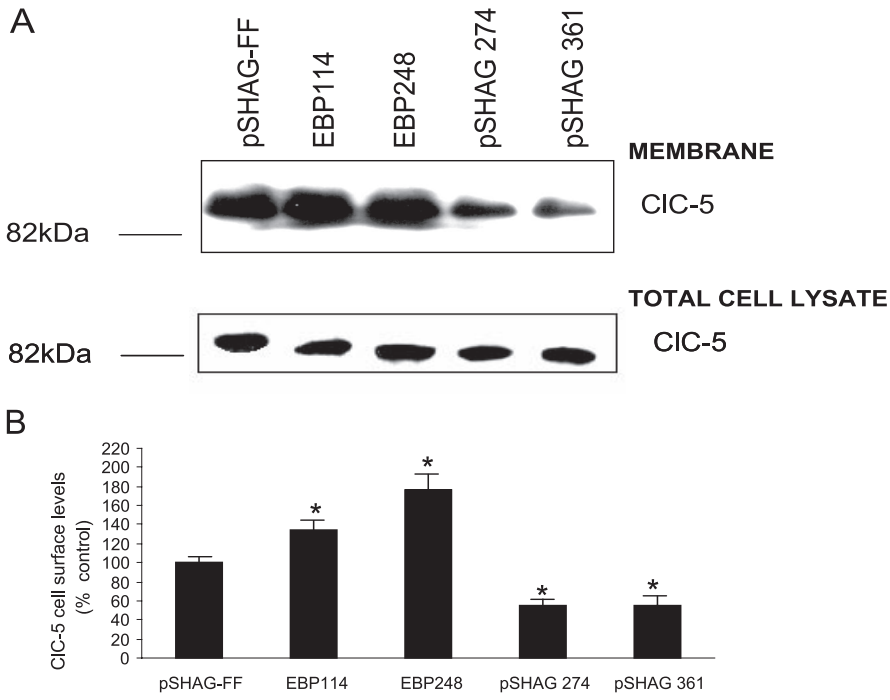


FIGURE 8. **Silencing NHERF1 and NHERF2 alters the cell-surface amount of ClC-5.** *A*, representative Western blot showing the effect of silencing NHERF1/2 on the levels of cell-surface ClC-5. OK cells were transfected with either NHERF1 EBP114 and EBP248 or pSHAG274 and pSHAG361 to silence NHERF1 or NHERF2, respectively. The cell-surface biotinylated fractions were harvested and Western blotted using ClC-5 antibody. Under all conditions, the level of ClC-5 in the total cell lysate was unaltered. *B*, *bar graph* showing the levels of ClC-5 at the cell-surface fraction. Silencing NHERF1 resulted in a significant increase in ClC-5 (156 ± 14% and 193 ± 21% of control; $n = 3$; *, $p < 0.05$). In contrast, silencing NHERF2 significantly decreased the levels of ClC-5 to 52 ± 6% and 62 ± 10% of control ($n = 3$; *, $p < 0.05$).

uptake by OK cells is inhibited by cAMP, an effect that has been attributed to inhibition of NHE3 (11). We therefore investigated whether 8-Br-cAMP could inhibit the increase in albumin uptake observed following silencing of NHERF1. Despite the 20% increase in albumin uptake, the percentage inhibition of albumin uptake by 8-Br-cAMP remained unchanged at 21.9 ± 3% and 21.8 ± 3% ($n = 3$) in cells transfected with pSHAG or EBP114, a value that was not significantly different from untransfected cells (Fig. 6*C*).

We then used confocal microscopy to confirm the changes in albumin uptake in response to silencing NHERF1/2 using previously described methods. OK cells co-transfected with GFP and the silencing plasmids were exposed to TR-albumin, and the fixed cells were examined by dual-wavelength confocal microscopy. Albumin is taken up into endocytic vesicles that can be readily visualized at the plane of the apical membrane and quantitated. In control cells there was an average of 18 ± 1 vesicles per cell, which were standardized to 100% (Fig. 7, *A* and *B*, $n = 30$ cells from three separate experiments). In cells where NHERF1 was silenced by transfection with EBP114 and EBP248 there was a significant increase in the number of endocytic vesicles to 136.9 ± 0.9% and 126.3 ± 1.05% of control, respectively (Fig. 7, *A* and *B*, $n = 3$, $p < 0.05$). In contrast, silencing NHERF2 by transfection with pSHAG274 and pSHAG361 resulted in a pronounced decrease in albumin containing endocytic vesicles to 23.7 ± 0.5% and 35.4 ± 0.8% of control, respectively (Fig. 7, *A* and 7*B*, $n = 30$ cells from three separate experiments, $p < 0.05$). These data obtained in single cells confirm the effects observed using albumin uptake in entire monolayers of transfected cells.

*Effect of Silencing NHERF1/2 on Cell-Surface Levels of ClC-5*—The availability of ClC-5 to the endocytic complex is a limiting factor for albumin uptake, therefore the decrease in albumin uptake when NHERF2 is silenced should be paralleled by a decrease in the surface levels of ClC-5. Indeed, silencing NHERF2 with either pSHAG274 or pSHAG361 resulted in a significant decrease in ClC-5 at the cell surface (Fig. 8, *A* and *B*, 52 ± 6% and 62 ± 10%, respectively), compared with the pSHAG control ($n = 4$, $p < 0.05$). Conversely, the increase in albumin uptake due to silencing of NHERF1 should be paralleled by an increase in cell-surface levels of ClC-5. When cells were transfected with either EBP114 or EBP248 to silence NHERF1, we observed a significant increase in cell-surface levels of ClC-5 (Fig. 8, *A* and *B*, 156 ± 14% and 193 ± 21%, respectively) compared with pSHAG control ($n = 3$, $p < 0.05$). Under the different conditions, there was no change in the total amount of ClC-5 in the cell lysate (Fig. 8*A*).

*Membrane Association of NHERF1 and NHERF2 in Response to Albumin*—Both NHERF1 and NHERF2 are abundant in the cytoplasm and must be recruited to the cell membrane as required. Our model predicts that more NHERF2 should associate with the membrane in the presence of albumin to facilitate the assembly of the endocytic complex in parallel with the increase in ClC-5 that we have previously demonstrated (36). If NHERF1/2 physically associate with the plasma membrane then they should be detected in association with cell-surface proteins. We therefore performed surface biotinylation of OK cells after treating the cells in the presence or absence of a normal tubular concentration of albumin (10 μg/ml) for 2 h at 37 °C. Biotinylated proteins were then isolated after cell lysis, and the association of NHERF1/2 with biotinylated plasma membrane proteins was determined by Western blotting. Densitometric analyses of the Western blots revealed (Fig. 9, *A* and *B*) that albumin caused a significant increase in NHERF2 associated with cell-surface proteins (125.0 ± 5.2% of control levels, $n = 3$, $p < 0.05$). In contrast, the levels of NHERF1 were significantly decreased to 67.0 ± 7.2% of control levels ($n = 3$, $p < 0.05$) following exposure to albumin. Importantly, there was no change in the levels of either NHERF1 or NHERF2 in the total cell lysate (Fig. 9*A*).

Recruitment of NHERF1/2 to the plasma membrane typically involves association with ezrin via the C-terminal ezrin binding domain (24). We therefore investigated the effects of deleting the ezrin binding domains (ΔEZR) of NHERF1 and NHERF2 on albumin uptake. Overexpression of NHERF1ΔEZR resulted in significant increases in albumin uptake (Fig. 9*C*, 124.3 ± 2.3%, $n = 3$, $p < 0.05$). In contrast NHERF2ΔEZR significantly reduced albumin uptake to 80.3 ± 3.9% of control levels ($n = 3$, $p < 0.05$).

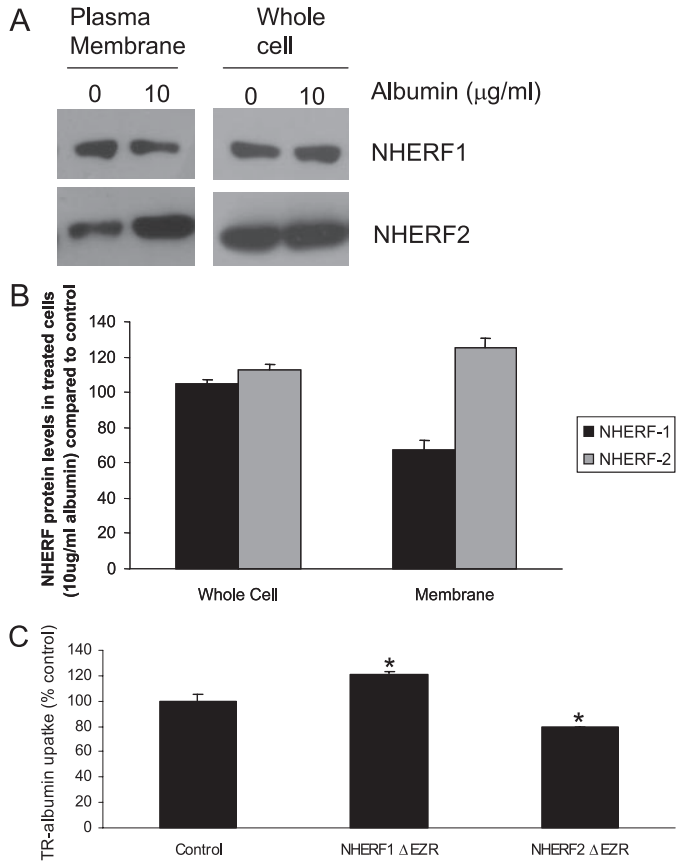


FIGURE 9. **Albumin alters the levels of NHERF1/2 associated with the cell surface.** OK cells were exposed to albumin (10 μg/ml) for 2 h at 37 °C, and the cell-surface-associated fraction was isolated using surface biotinylation. *A*, representative Western blot showing the changes in cell-surface-associated NHERF1/2 in response to treatment with albumin. However, the level of NHERF1 and NHERF2 in the total cell lysate was unaltered. *B*, *bar graph* showing that, in the presence of albumin, the levels of NHERF1 associated with the plasma membrane were significantly decreased (67 ± 7.2%; $n = 3$; *, $p < 0.05$) compared with cells not exposed to albumin. In contrast, NHERF2 levels significantly increased at the cell surface compared with control (125 ± 5.2%; $n = 3$; *, $p < 0.05$). However, the level of NHERF1 and NHERF2 in the total cell lysate was unaltered. *C*, *bar graph* showing the effects of overexpression of ezrin binding-deficient NHERF1/2 on albumin uptake. In cells overexpressing NHERF1ΔEZR, albumin uptake was increased to 124.3 ± 2.3% ($n = 3$; *, $p < 0.05$). In contrast, when NHERF2ΔEZR was overexpressed albumin uptake was significantly reduced (80.3 ± 3.9%; $n = 3$; *, $p < 0.05$).

## DISCUSSION

It is increasingly clear that the obligate role of ClC-5 in albumin uptake involves the assembly of the albumin endocytic complex and its association with the cytoskeleton (21, 22, 48). In the current study, we have started to address the protein-protein interactions involved in this process and focus on the role of NHERF PDZ scaffolds. We reveal a novel role for NHERF2 in albumin uptake by OK cells that is mediated by direct interaction with ClC-5. We also show that NHERF1 in the microvillus can influence the rate of albumin uptake, possibly by both limiting the availability of NHE3 to the albumin endocytic compartment and altering cell-surface levels of ClC-5.

OK cells are the accepted cell culture model for albumin uptake by the proximal tubule. Compared with the native proximal tubule, OK cells do not have a dense brush border, and their intravillar regions are less morphologically complex (49). However, they retain megalin/ClC-5- and NHE3-dependent albumin uptake pathways (36, 50), and NHE3 is reported to traffic from the microvilli to the intravillar regions (34). Importantly, the distribution of NHERF1 in the microvilli domain and NHERF2 in regions between the microvilli that we report corresponds to their distributions in the mouse and human proximal tubules (29, 31), thus OK cells are a suitable model for the investigation of the molecular basis of receptor-mediated albumin uptake (see Ref. 2). Many studies investigating the role of NHERF1/2 and NHE3 in OK cells rely on overexpression of these proteins (34, 51). It is important to note that the current study was performed using OK cells that endogenously express NHERF2. Thus, these data reflect genuine protein interactions under native conditions.

ClC-5 co-immunoprecipitated NHERF2 but not NHERF1 from OK cell lysate. This is consistent with the spatial heterogeneity of ClC-5 and NHERF1 in the proximal tubule. Although ClC-5 co-localizes with albumin in OK cells and Rab4 in recycling endosomes (46), NHERF1 is present at the microvillus (31), thus it is unlikely that these two proteins interact *in vivo*. ClC-5 binds the PDZ2 module of NHERF2, and the binding does not involve the final amino acids *ESIL*FN at the C terminus. This indicates that, similar to NHE3, ClC-5 interacts with NHERF2 via an internal binding site (20). The fact that NHERF2 had no effect on ClC-5 current magnitude in *Xenopus* oocytes argues against the NHERF2-ClC-5 complex dimerizing to increase the cell-surface density of ClC-5, as has been reported for NHERF1 and CFTR (52). Alternatively, NHERF2 may act to stabilize ClC-5 at the cell membrane in a cell-type-specific manner involving interacting proteins that are not present in oocytes.

Albumin uptake involves interactions with the cytoskeleton (6, 23) and increases both the cell-surface levels of ClC-5 (36) and the number of actin clusters at the apical membrane (21). We now show that the presence of albumin also increases the levels of NHERF2 associated with the plasma membrane. Furthermore, silencing NHERF2 caused significant reductions in surface ClC-5, the number of actin clusters, and albumin uptake. Under conditions where albumin uptake is reduced, one prediction would be a reduced rate of internalization of ClC-5 paralleled by an increased residence time of ClC-5, reflected by an increase in surface expression. The fact that we see a reduction in the degree of albumin uptake and surface ClC-5 suggests that an accessory protein such as NHERF2 is required to maintain ClC-5 at the membrane. Taken together these data support a model in which ClC-5 plays a key role in nucleating the formation of the endocytic complex, presumably by mechanisms that involve tethering of the complex via NHERF2 to the actin cytoskeleton. The inhibition of albumin uptake upon overexpression of an ezrin binding-deficient NHERF2 further demonstrates the importance of the interaction between NHERF2 and ezrin interaction in this process.

It has been suggested that increased levels of cAMP reduce albumin uptake by inhibiting NHE3 (11). cAMP inhibits NHE3 via an NHERF1-ezrin-protein kinase A complex (53) and basal level phosphorylation of NHE3 by protein kinase A is reported in proximal tubule cells (54). Therefore, we initially attributed the increase in albumin uptake following silencing of NHERF1 to disruption of the normal interaction between NHERF1-ezrin and protein kinase A, leading to a reduction in the tonic inhibition of NHE3. Silencing NHERF1, however, did not prevent the cAMP-mediated inhibition of albumin uptake, indicating that this effect of cAMP does not involve NHERF1. The fact that NHERF1 is restricted to the microvilli and not present at the site of albumin uptake is consistent with this result. Furthermore, there are no reports of albuminuria in NHERF1 knock-out mice. Finally, baseline NHE3 activity in OK cells is not altered by overexpression of an ezrin binding-deficient NHERF1 (55), which also argues against tonic inhibition of NHE3 affecting albumin uptake. Thus, our findings show that cAMP does not decrease albumin uptake in OK cells by inhibiting NHE3 via NHERF1.

How else could silencing of NHERF1 increase albumin endocytosis? NHE3 has a key role in albumin uptake, and, similar to ClC-5, its availability to the endocytic complex must be a limiting step in albumin uptake. In OK cells, NHE3 traffics from the microvillus to the intravillar cleft (34). It has been suggested that stimulated endocytosis may require changes in the mobility of NHE3 by mechanisms that involve NHERF1/2 (34). Importantly, at the microvillar membrane, a significant fraction of NHE3 is immobilized; that is, it is tethered to the actin cytoskeleton via proteins such as NHERF1 or small GTPases (33, 34). Based on these data, we can propose a model in which silencing NHERF1 simply increases the mobile fraction of NHE3 available to the intravillar cleft, thereby accelerating albumin uptake. Albumin also caused a significant reduction in plasma membrane-associated NHERF1 possibly allowing increased mobility of NHE3. Similarly, the ezrin binding-deficient NHERF1 may be exerting a dominant negative effect on the normal tethering of NHE3 to the cytoskeleton thereby increasing its mobility. The link between NHERF1 and albumin uptake was further strengthened by the increase in cell-surface ClC-5 observed when NHERF1 was silenced. Our model predicts that, as an essential component of the endocytic complex, the increase in albumin uptake must be accompanied by a parallel increase in ClC-5. Conversely, in cells where NHERF2 is silenced, ClC-5 levels are reduced as less of the endocytic complex is formed.

The data from the current study clearly support a model in which the rate of albumin endocytosis is governed by the availability of key proteins that constitute the endocytic complex. At the plasma membrane, ClC-5 acts as a key structural element in the macromolecular endocytic complex independent of any ion transporting activity. This is particularly relevant given the recent findings that ClC-5 functions as a $Cl^-/H^+$ antiporter rather than a $Cl^-$ channel (16, 17), which raise some questions as to the role of ClC-5 as an anion shunt in the albumin uptake process. Our data show how PDZ scaffolds can direct the activity of spatially discrete functional compartments within the apical domain of epithelial cells. Albumin increases the association of NHERF2 with the plasma membrane, where it links ClC-5 to ezrin to anchor the endocytic complex. In contrast, NHERF1 possibly plays a negative regulatory role in controlling the availability of NHE3 to the endocytic complex. Albumin reduces the association of NHERF1 with the plasma membrane, which could increase availability of NHE3 to the endocytic compartment and thereby increase levels of ClC-5 and albumin uptake. It remains to be determined whether ClC-5 and NHE3 are present in the same macromolecular complex. It is possible that NHERF2 could dimerize and link ClC-5 and NHE3. However, it has been shown that megalin and NHE3 interact via their C termini (56), and as a result, megalin may obscure the internal NHERF binding site on NHE3. It is also possible that another albumin uptake compartment exists that depends on NHE3 but not ClC-5 (48). Further biochemical/biophysical studies are required to elucidate the exact protein-protein interactions that mediate the formation of the albumin endocytic complex. In conclusion, our data suggest that albumin initiates the formation of the macromolecular complex that mediates its own internalization. This study highlights novel roles for the PDZ scaffolds NHERF1/2 in the constitutive uptake of albumin by the proximal tubule and extends our understanding of the molecular basis for the obligate role of ClC-5 in this process. From a clinical perspective, such data provide a mechanism that links NHE3 activity and mobility directly to albumin uptake, an issue that is relevant in terms of the $Na^+$ retention and proteinuria that frequently occurs in kidney diseases such as diabetic nephropathy (57, 58).

*Acknowledgments—We thank Prof. David Adams (School of Biomedical Sciences, University of Queensland, Australia) in whose laboratory the oocyte experiments were performed and Prof. David Cook (Dept. of Physiology, University of Sydney, Australia) to whom we are indebted for helpful discussions. We thank Prof. Olivier Devuyst (Universite Catholique de Louvain, Belgium) for the anti-ClC-5 antibody. Finally, we are grateful for the excellent research assistance of Sarah-Jane Conroy.*

## REFERENCES

1. Maack, T. (2000) *The Kidney: Physiology and Pathophysiology*, 3rd Ed. (Seldin, D. W., and Giebisch, G. eds) pp. 3005–3038, Lippincott Williams & Wilkins, New York
2. Gekle, M. (2005) *Annu. Rev. Physiol.* **67,** 573–594
3. Norden, A. G. W., Lapsley, M., Lee, P. J., Pusey, C. D., Scheinman, S. J., Tam, F. W. K., Thakker, R. V., Unwin, R. J., and Wrong, O. (2001) *Kidney Int.* **60,** 1885–1892
4. Christensen, E. I., and Birn, H. (2001) *Am. J. Physiol.* **280,** F562–F573
5. Czekay, R. P., Orlando, R. A., Woodward, L., Lundstrom, M., and Farquhar, M. G. (1997) *Mol. Biol. Cell* **8,** 517–532
6. Hryciw, D. H., Ekberg, J., Pollock, C. A., and Poronnik, P. (2006) *Int. J. Biochem. Cell Biol.* **38,** 1036–1042
7. Marshansky, V., Ausiello, D. A., and Brown, D. (2002) *Curr. Opin. Nephrol. Hypertens.* **11,** 527–537
8. Birn, H., Fyfe, J., Jacobsen, C., Mounier, F., Verroust, P., Ørskov, H., Willnow, T., Moestrup, S., and Christensen, E. (2000) *J. Clin. Invest.* **100,** 1353–1361
9. Gekle, M., Drumm, K., Mildenberger, S., Freudinger, R., Gassner, B., and Silbernagl, S. (1999) *J. Physiol.* **520,** 709–721
10. Gekle, M., Freudinger, R., and Mildenberger, S. (2001) *J. Physiol.* **531,** 619–629
11. Gekle, M., Serrano, O. K., Drumm, K., Mildenberger, S., Freudinger, R., Gassner, B., Jansen, H. W., and Christensen, E. I. (2002) *Am. J. Physiol.* **283,** F549–F558
12. Gekle, M., Volker, K., Mildenberger, S., Freudinger, R., Shull, G. E., and Wiemann, M. (2004) *Am. J. Physiol.* **287,** F469–F473
13. Lloyd, S. E., Pearce, S. H., Fisher, S. E., Steinmeyer, K., Schwappach, B., Scheinman, S. J., Harding, B., Bolino, A., Devoto, M., Goodyer, P., Rigden, S. P., Wrong, O., Jentsch, T. J., Craig, I. W., and Thakker, R. V. (1996) *Nature* **379,** 445–449
14. Wang, S. S., Devuyst, O., Courtoy, P. J., Wang, X. T., Wang, H., Wang, Y., Thakker, R. V., Guggino, S., and Guggino, W. B. (2000) *Hum. Mol. Genet* **9,** 2937–2945
15. Piwon, N., Gunther, W., Schwake, M., Bosl, M. R., and Jentsch, T. J. (2000) *Nature* **408,** 369–373
16. Picollo, A., and Pusch, M. (2005) *Nature* **436,** 420–423
17. Scheel, O., Zdebik, A. A., Lourdel, S., and Jentsch, T. J. (2005) *Nature* **436,** 424–427
18. Christensen, E. I., Devuyst, O., Dom, G., Nielsen, R., Van der Smissen, P., Verroust, P., Leruth, M., Guggino, W. B., and Courtoy, P. J. (2003) *Proc. Natl. Acad. Sci. U. S. A.* **100,** 8472–8477
19. Moulin, P., Igarashi, T., Van Der Smissen, P., Cosyns, J., Verroust, P., Thakker, R., Scheinman, S. J., Courtoy, P. J., and Devuyst, O. (2003) *Kidney Int.* **63,** 1285–1295
20. Yun, C. C., Lamprecht, G., Forster, D. V., and Sidor, A. (1998) *J. Biol. Chem.* **273,** 25856–25863
21. Hryciw, D. H., Pollock, C. A., and Poronnik, P. (2005) *Am. J. Physiol.* **288,** F1227–F1235
22. Hryciw, D. H., Wang, Y. H., Devuyst, O., Pollock, C. A., Poronnik, P., and Guggino, W. B. (2003) *J. Biol. Chem.* **278,** 40169–40176
23. Gekle, M., Mildenberger, S., Freudinger, R., Schwerdt, G., and Silbernagl, S. (1997) *Am. J. Physiol.* **272,** F668–F677
24. Shenolikar, S., Voltz, J. W., Cunningham, R., and Weinman, E. J. (2004) *Physiology* (*Bethesda*) **19,** 362–369
25. Weinman, E. J., Steplock, D. A., Wang, Y., and Shenolikar, S. (1995) *J. Clin. Invest.* **95,** 2143–2149
26. Yun, C. H., Oh, S., Zizak, M., Steplock, D., Tsao, S., Tse, C. M., Weinman, E. J., and Donowitz, M. (1997) *Proc. Natl. Acad. Sci. U. S. A.* **94,** 3010–3015
27. Hernando, N., Wagner, C. A., Gisler, S. M., Biber, J., and Murer, H. (2004) *Curr. Opin. Nephrol. Hypertens.* **13,** 569–574
28. Lau, A. G., and Hall, R. A. (2001) *Biochemistry* **40,** 8572–8580
29. Weinman, E. J., Lakkis, J., Akom, M., Wali, R., Drachenberg, C., Coleman, R. A., and Wade, J. B. (2002) *Pathobiology* **70,** 314–323
30. Wade, J. B., Welling, P. A., Donowitz, M., Shenolikar, S., and Weinman, E. J. (2001) *Am. J. Physiol.* **280,** C192–C198
31. Wade, J. B., Liu, J., Coleman, R. A., Cunningham, R., Steplock, D. A., Lee-Kwon, W., Pallone, T. L., Shenolikar, S., and Weinman, E. J. (2003) *Am. J. Physiol.* **285,** C1494–C1503
32. Thelin, W., Hodson, C., and Milgram, S. (2005) *J. Physiol.* **567,** 13–19
33. Alexander, R. T., Furuya, W., Szaszi, K., Orlowski, J., and Grinstein, S. (2005) *Proc. Natl. Acad. Sci. U. S. A.* **102,** 12253–12258
34. Cha, B., Kenworthy, A., Murtazina, R., and Donowitz, M. (2004) *J. Cell Sci.* **117,**

3353–3365
35. Lamprecht, G., Weinman, E. J., and Yun, C. H. (1998) *J. Biol. Chem.* **273,** 29972–29978
36. Hryciw, D. H., Ekberg, J., Lee, A., Lensink, I. L., Kumar, S., Guggino, W. B., Cook, D. I., Pollock, C. A., and Poronnik, P. (2004) *J. Biol. Chem.* **279,** 54996–55007
37. Yun, C. C., Chen, Y., and Lang, F. (2002) *J. Biol. Chem.* **277,** 7676–7683
38. Hryciw, D. H., Rychkov, G., Hughes, B., and Bretag, A. (1998) *J. Biol. Chem.* **273,** 4304–4307
39. Liou, W., Geuze, H. J., and Slot, J. W. (1996) *Histochem. Cell Biol.* **106,** 41–58
40. Paddison, P., Caudy, A., Bernstein, E., Hannon, G., and Conklin, D. (2002) *Genes Dev.* **15,** 948–958
41. Lee, E. M., Pollock, C. A., Drumm, K., Berden, J., and Poronnik, P. (2003) *Am. J. Physiol.* **285,** F748–F757
42. Drumm, K., Lee, E., Stanners, S., Gassner, B., Gekle, M., Poronnik, P., and Pollock, C. A. (2003) *Cell Physiol. Biochem.* **13,** 199–206
43. Drumm, K., Bauer, B., Freudinger, R., and Gekle, M. (2002) *Cell Physiol. Biochem.* **12,** 187–196
44. Hernando, N., Deliot, N., Gisler, S. M., Lederer, E., Weinman, E. J., Biber, J., and Murer, H. (2002) *Proc. Natl. Acad. Sci. U. S. A.* **99,** 11957–11962
45. Biemesderfer, D., Rutherford, P., Nagy, T., Pizzonia, J., Abu-Alfa, A., and Aronson, P. (1997) *Am. J. Physiol.* **273,** F289–F299
46. Devuyst, O., Christie, P. T., Courtoy, P. J., Beauwens, R., and Thakker, R. V. (1999) *Hum. Mol. Genet.* **8,** 247–257
47. Yun, C. C., Sun, H., Wang, D., Rusovici, R., Castleberry, A., Hall, R. A., and Shim, H. (2005) *Am. J. Physiol.* **289,** C2–C11
48. Wang, Y., Cai, H., Cebotaru, L., Hryciw, D. H., Weinman, E. J., Donowitz, M., Guggino, S. E., and Guggino, W. B. (2005) *Am. J. Physiol.* **289,** F850–F862
49. McDonough, A. A., and Biemesderfer, D. (2003) *Curr. Opin. Nephrol. Hypertens.* **12,** 533–541
50. Gekle, M., Mildenberger, S., Freudinger, R., and Silbernagl, S. (1996) *Am. J. Physiol.* **271,** F286–F291
51. Weinman, E. J., Steplock, D., Wade, J. B., and Shenolikar, S. (2001) *Am. J. Physiol.* **81,** F374–F380
52. Li, J., Dai, Z., Jana, D., Callaway, D., and Bu, Z. (2005) *J. Biol. Chem.* **280,** 37634–37643
53. Weinman, E. J., Steplock, D., and Shenolikar, S. (2003) *FEBS Lett.* **536,** 141–144
54. Kocinsky, H., Girardi, A., Biemesderfer, D., Nguyen, T., Mentone, S., Orlowski, J., and Aronson, P. (2005) *Am. J. Physiol.* **289,** F249–F258
55. Weinman, E. J., Steplock, D., Wade, J. B., and Shenolikar, S. (2001) *Am. J. Physiol.* **281,** F374–F380
56. Biemesderfer, D., DeGray, B., and Aronson, P. S. (2001) *J. Biol. Chem.* **276,** 10161–10167
57. Hryciw, D. H., Lee, E. M., Pollock, C. A., and Poronnik, P. (2004) *Clin. Exp. Pharmacol. Physiol.* **31,** 372–379
58. Remuzzi, G., Schieppati, A., and Ruggenenti, P. (2002) *N. Engl. J. Med.* **346,** 1145–1151

# Regulation of Albumin Endocytosis by PSD95/Dlg/ZO-1 (PDZ) Scaffolds: INTERACTION OF Na+-H+ EXCHANGE REGULATORY FACTOR-2 WITH ClC-5

Deanne H. Hryciw, Jenny Ekberg, Charles Ferguson, Aven Lee, Dongsheng Wang, Robert G. Parton, Carol A. Pollock, Chris C. Yun and Philip Poronnik

*J. Biol. Chem. 2006, 281:16068-16077.*
*doi: 10.1074/jbc.M512559200 originally published online April 6, 2006*

---